Concentrated solar power applied to desalination

Camila COHEN[1], Flora WALLERANT[1], Dylan LORFING[2], Quentin FALCOZ[3], Régis OLIVES[3*]

[1]Processes, Materials and Solar Energy Laboratory, PROMES-CNRS, 7 Rue du Four Solaire, 66120, Font-Romeu, France
[2]TBI, Université de Toulouse, CNRS, INRAE, INSA, 135 Avenue de Rangueil, 31077, France
[3]PROMES-CNRS, Université de Perpignan Via Domitia, Tecnosud, Perpignan 66100, France
[*](Corresponding author: regis.olives@promes.cnrs.fr)

Abstract - Desalination is a possible solution to global water scarcity. Nevertheless, it is highly energy consuming and thus polluter. A concentrated solar desalination device is studied. It consists in a solar furnace concentrating solar power on a receiver. The receiver, immersed in water, heats it until it boils. In order to avoid fouling, the process is done in a film boiling regime. Different power values were applied to study the vapor film's setting. It was observed that after its establishment, the power could be decreased without it vanishing. Results also show the protective effect of the vapor film against fouling.

1. Introduction

Only 1 % of Earth's water is available for human consumption. Socio-cultural, and economic disparities exist, as well as enormous gaps between different countries and/or regions. This global problem is of big concern as water scarcity threatens human activities and human health. The majority of Earth's water (up to 97 %) resides in the ocean, thus being saline water, making it not usable for the majority of human requirements (drinking, food production, irrigation...), unless it goes through a desalination process (removing excess salts and other dissolved chemicals). In light of this vast amount, desalination looks like the perfect solution to cope with waterscarcity.

Desalination's cost is based on various elements: the interest rates and life expectancy of the equipment, the investment expenses, the required labour or other operation costs. However, its cost sees an important rise, which shows a direct connection with the energy market. Desalination's price fluctuation depends the most (up to 25 %) on the price of energy [1]. These leads toa great amount of regions not having access to water due to economic unaffordability.

If seawater desalination has proven its efficiency, it is an energy consuming solution. In addition, thermal and electrical energy, based for the great majority on the consumption of fossil fuel, are the most used by industrial desalination sites. To overcome this drawback, renewable energy systems have been developed to power desalination plants [2]. The use of alternative energy for desalination [3] copes with the cost of energy as well as the production of greenhouse gases. Furthermore, water is essential in providing energy, just as energy is needed to provide water, as the energy industry consumes important amounts of water in each one of its stages. Neglecting the energy-related water use can result in higher emissions. Their linkage relationship must be taken into account when identifying energy mix scenarios that fit best the environment, and water and energy supply stress.

Moreover, desalination technologies have to cope with some inconveniences. The most disadvantageous is salt accumulation on the desalination equipment's walls that are in contact with saline water. The salt accumulation leads to corrosion of the equipment, increased and very

https://doi.org/10.25855/SFT2023-082

frequent maintenance and thus a shortening of its lifetime. Also, the build-up blocks heat exchange with seawater, therefore reducing the operational efficiency [4].

There are two major technologies regarding solar energy. Photovoltaic, which directly converts solar radiation into electricity, and concentrated solar technology which converts solar radiation both into heat and electricity. The key advantages of concentrated solar technology over photovoltaics is its capability to store heat energy. This makes the system continuously efficient, since the storage can be used during absences of sunlight, thus overcoming the limitations of the intermittent nature of solar energy [5].

Concentrated solar power (CSP) can fuel a desalination plant, either directly by using the heat produced when concentrating the solar irradiation to boil water, or indirectly by producing electricity to power the desalination plant. The use of CSP for desalination was first introduced in 2002 by Blanco *et al.* [6]. Afterwards, this technology has been continuously investigated in order to make it commercial and economical [7]. The other advantage of solar concentration is that it can reach high temperatures. At sufficiently high temperatures, it is possible to generate a film of vapor that will protect the surfaces of the system and thus avoid salt deposits. The advantages and disadvantages of CSP for desalination were presented by Lorfing *et al.* [8]. In this context a direct and integrated concentrated solar power desalination device has been elaborated in Odeillo's solar furnace research laboratory.

2. Experimental device

2.1. Experimental set-up

The experimental set-up consists in a solar furnace which concentrates solar power on a receiver placed at its focal point. This last one, immersed in water, takes it to boiling point. Figure 1 shows a schema of the vertical solar furnace.

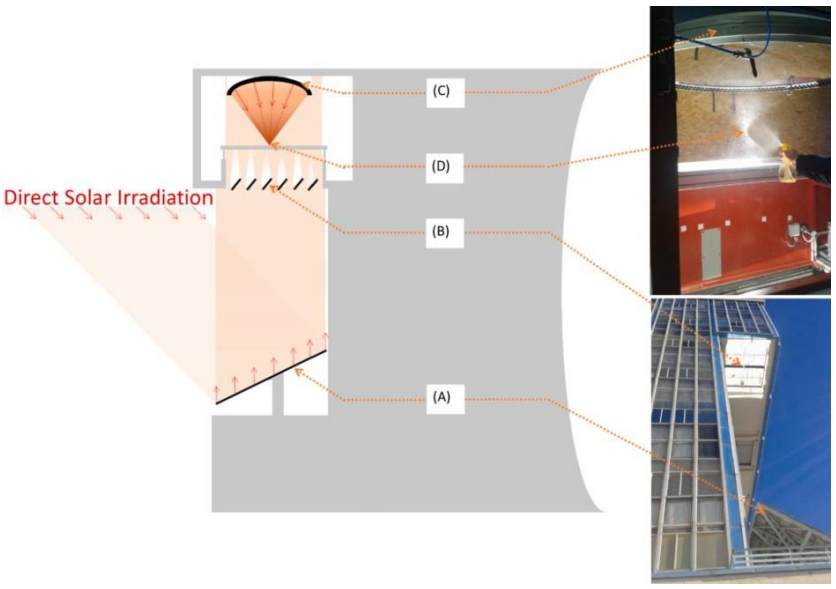

Figure 1 : *Layout of the solar vertical concentrator installation at the Odeillo solar furnace in France showing (A) the heliostat, (B) the carbon blade shutter, (C) the parabolic reflector, and (D) the focal point[8,9]*

A parabolic dish technology was implemented. Direct solar irradiation was directed towards a parabola by means of a heliostat (A). The amount of radiation arriving on the parabola is controlled thanks to carbon blade shutters (B). The parabola (C) (1.5 m of diameter) concentrates solar irradiation on a receiver placed at its focal point (D). This last one is in contact with water that evaporates as the receiver is heated. We can follow the Nukiyama's boiling curve [10]. The process took place at a particular boiling regime called film boiling, where a sudden increase in temperature between the heated wall and the fluid being heated leads to a boiling crisis, and thus to the formation of a vapor film around theheated surface.

The experimental set-up is shown in figure 2.

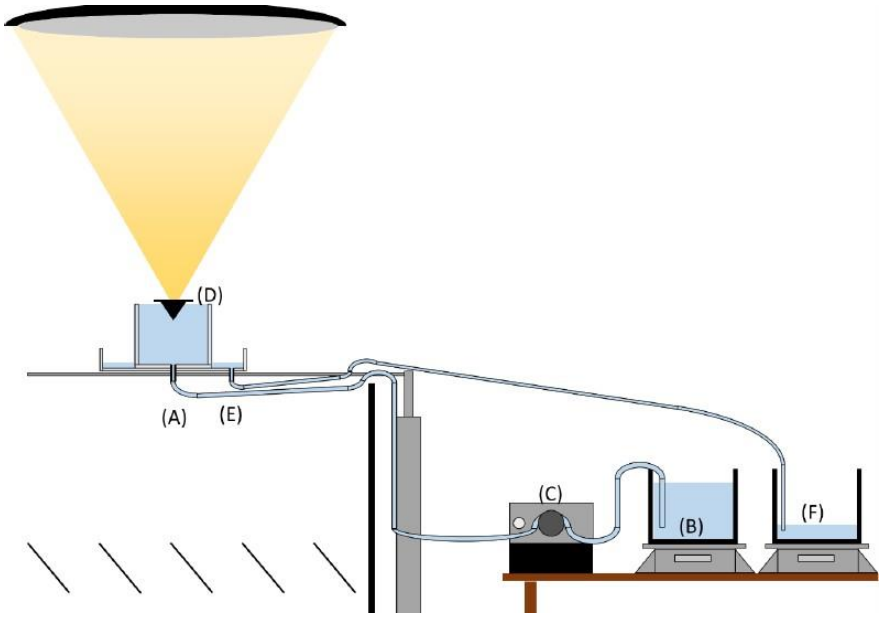

Figure 2 : *Fluids circulation in the experimental set-up[9]*

The receiver (D) consists in a cone and a circular disc at its base (40 mm of external diameter). The conical shape was chosen for two reasons. First, it allows to create a cavity on the upper side that traps solar energy increasing the efficiency of the system. Second, it allows to guide the vapor film to the receiver's edges, facilitating its extraction. The disc was chosen to fixate the cone to the rest of the set-up. The receiver is immersed in water contained in a main tank, arriving there thought an inlet (A) from a weighted tank (B). Its circulation is ensured by aperistaltic pump (C), allowing to regulate precisely the flow. Once in the main tank, part of theliquid is vaporized, and the vapor thus produced is evacuated into the atmosphere. The vapor'scollection was not studied. The part of the liquid not vaporized reaches the secondary tank by overflow. An outlet at the bottom of the secondary plexiglass tank (E) allows the evacuation of the liquid collected in a recovery tank (F). The secondary water tank (25 x 25 cm) is small enough to avoid too much shading.

2.2. Different materials for the receivers

Different receivers made of three different materials and geometries were tested. The table 1 summarizes them (average conductivity coefficients are given). Steel and cast iron were chosen for their high melting temperature (needed in light of the power values used). Copper

was chosen for its high conductivity coefficient, as the concentrated solar power heats the upper side of the receiver, conduction leads to the lower side heating andthus the boiling of water. The different geometries were chosen to test the design impact on the vapor film creation and evacuation.

Material	**Melting temperature (°C)**	**Average conductivity ($W.m^{-1}.K^{-1}$)**	**Half aperture angle (°)**	**Internal Diameter (mm)**	**emissivity**
Steel	1400	25	30 45 60	21 25 30	~0.85
Cast Iron	1250	50	30 45 60	21 25 30	~0.8
Copper	1085	400	30 45 60	21 25 30	~0.8

Table 1: *Receivers tested with their material and geometry information*

The emissivity of the materials is initially that of the unoxidised metal and tends to increase during the experiments. It is therefore between 0.75 and 0.85.

2.3. Instrumentation

Temperatures are measured thanks to K-type thermocouples. Figure 3 shows their location.

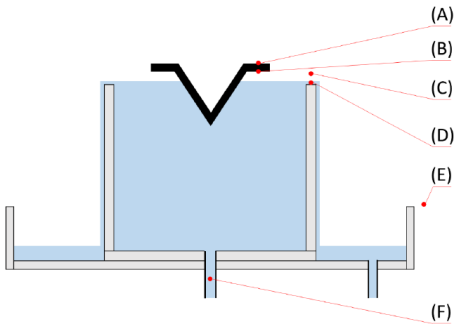

Figure 3: *Thermocouples' locations*

The acquired temperatures are: the receiver's upper and lower surface temperatures (A and B respectively), the outlet vapor temperature (C), the outlet and inlet water temperatures (D and F respectively) and the ambient temperature (E). The acquisition is ensured by a Midi LOGGER GL240 recorder from Graphtec©.

The direct normal irradiation (DNI) measurement is performed by a pyrheliometer (Kipp & Zonen CHP1) and recorded by a 63 precision Gantner A4 acquisition module. They are installed in a meteorological station on the roof of the solar furnace.

Water flow rates are measured with digital acquisition scales: OHAUS brand Explorer (0.1 g resolution) and KERN FCB A (1 g resolution). The masses measured throughout the experiment are used to calculate the flow rate of the water inlet and outlet. The vapor flow rate is calculated by the difference of these two.

Finally, a Basler *acA*1920 150 μm CMOS camera coupled to a lens with a focal length of 35 mm allows visual monitoring of the submerged part of the receiver.

3. Results and discussion

The purpose of the experimental device is to demonstrate the feasibility of the concentrated solar evaporator system and the creation of the vapor film. The film boiling regime is generally avoided, because it creates a thermal resistance between the heated surface and liquid water. Special attention is given here, in order to study its ability to protect the receiver from fouling.

In order to reach these objectives, different experiments were performed. The supply tank is filled with enough water to ensure the operation throughout the experiments. The thermocouples are glued or welded to the receivers. The receiver is then positioned at the focal point of the concentrator. The pump is started to fill the main tank. A progressive opening of the regulation blades is done. The position of the evaporator is adjusted as required so that the focal spot is contained within the conical cavity of the receiver. Ambient temperature is measured around 17 °C. Once everything is in place, water starts to circulate with an average flow rate of 1.02 $10^{-3}\, kg\ s^{-1}$. Then different power levels are applied, thanks to the progressive opening of the carbon blades. This is done until the set of the vapor film. Afterwards, the blades are slowly shut until the film vanishes.

$\dot{Q}_{solar}$ is the solar power concentrated in the receiver. It is calculated thanks to the DNI, the blades aperture percentage x and the following correlation (with $DNI_{ref} = 1000\ W.m^{-2}$):

$$\dot{Q}_{solar} = (-3.166 \cdot 10^{-4} \cdot x^3 + 9.896 \cdot 10^{-2} \cdot x^2 + 1.769 \cdot x) \cdot \frac{DNI}{DNI_{ref}} \qquad (1)$$

The power transferred to the water will depend on the exchange surface, but also on the radiation and convection losses at the top surface of the receiver.

3.1. Vapor film creation

The camera allowed to observe the passage between the nucleate boiling regime to the filmboiling regime. Figure 4 shows different images of an immersed receiver through the experiment.

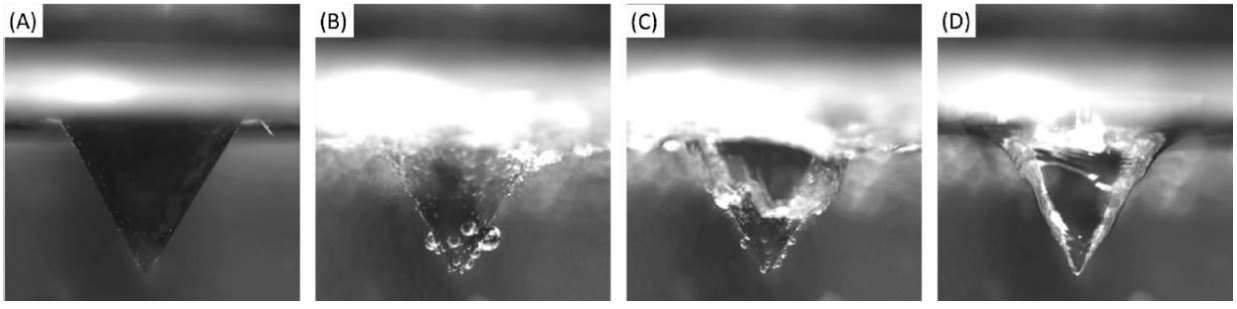

Figure 4: *Picture of the progressive setting of the vapor film. A: immersed receiver, B: nucleate boiling,C: film start, D: film installed*

Figure 5 shows the plot of $\dot{Q}_{solar}$, and the temperatures for the inlet water, outlet water and vapor as a function of time. Note that the incremental evolution of the solar flux is linked to the setting of the carbon blade shutters.

We observe nucleate boiling taken place first (B). Due to the location at high altitude of the lab, and measurement errors, the boiling point is measured around 95 ℃. Then, the boiling crisis takes place when the power is enough to go from nucleate boiling to film boiling. The film starts to set from the tip of the cone (C). The film apparition takes place at $\dot{Q}_{solar}$ between 700 W and 800 W for every receiver (D). The film vanishing value is around $\dot{Q}_{solar} = 300\ W$ for receivers in copper and $\dot{Q}_{solar} = 730\ W$ for receivers in steel. The cast iron experiments were interrupted so values were not determined. The reason of the interruption were heat problems: the receiver started melting when exposed to high $\dot{Q}_{solar}$.

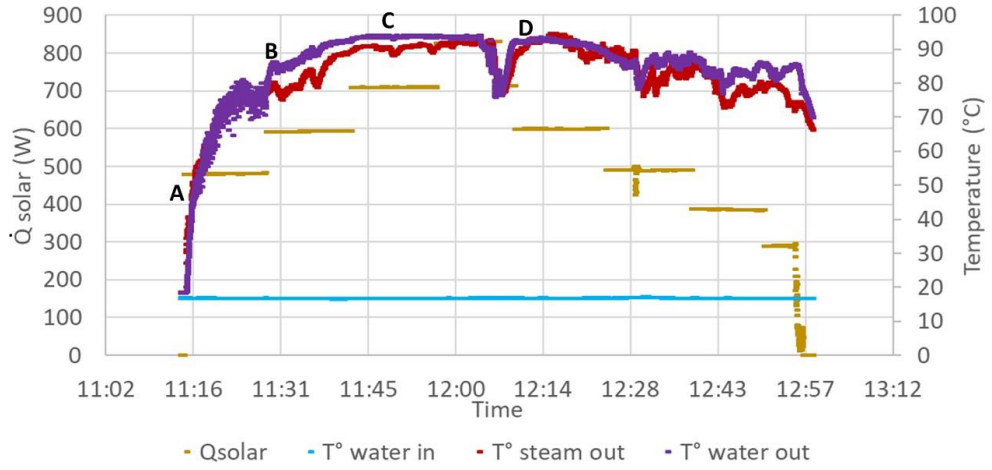

Figure 5: *Water temperatures as a function of the solar power (Copper-60 ° receiver). A: immersed receiver, B: nucleate boiling, C: film start, D: film installed*

The film proved to protect the wall of the receiver. In the case of an already fouled receiver, it also proved a clearing effect.

3.2. Conduction through the receiver

The performance of the receiver was evaluated comparing its upper and lower temperatures. This aims at evaluating the thermal conduction through its thickness, and thus the percentage of energy it transfers to the liquid. Figure 6 shows the variation over time of these temperatures, and the applied solar power.

As expected, temperatures increase with the solar power concentrated on the receiver. The important temperature rise around 12 : 50 is due to the boiling crisis. The film acts as insulator between the cone and water, leading the cone's temperature to higher values. The difference between temperatures on the lower and upper plate parts are due to the direct exposition to solar power on the upper side. The lower side receives heat only through conduction.

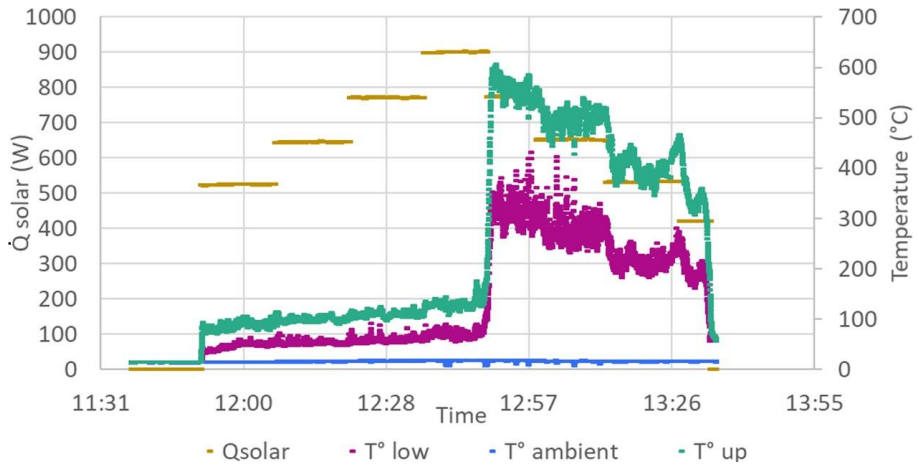

Figure 6: *Receiver temperatures as a function of the solar power (Copper-45 ° receiver).*

3.3. Performances

To compare each receiver's performance, we compare the energy needed to keep the vapor film in place. This is the lowest $\dot{Q}_{solar}$ before the film vanishes.

The table 2 gathers the lowest $\dot{Q}_{solar}$ before the film vanishes for different receivers. Because of the early interruption of the cast iron receiver's experiments, we do not have values for these receivers. Also, the value for the steel receiver of 30 ° half aperture angle gave incoherent results so it is not taken into account.

Material	**Half aperture angle (°)**	$\dot{Q}_{solar}$ **(W)**
Copper	30	275
	45	420
	60	246
Steel	45	738
	60	737

Table 2: *Lowest $\dot{Q}_{solar}$ before the film vanishes for different receivers*

The vapor film is stable for lower $\dot{Q}_{solar}$ values for the copper receivers. This means for these receivers lower energy is necessary to keep the film boiling regime. Performance is proportionate to $\dot{Q}_{solar}$, so we can deduct that copper receivers (of half aperture angle $= 30$; 60 °) are 2.7 and 3 times more efficient than steel receivers, respectively. As for the copper receiver (of half aperture angle $= 45$ °), its performance is 1.75 times higher.

4. Conclusion

Desalination can be a great solution to cope with water scarcity, but it is highly energy consuming process. In addition to this, the energy consumption has a significant effect on the planet. With recent global warming increase, the option to turn towards renewable energies should be studied. As regions with higher water scarcity are also those characterized by important solar irradiation, a concentrated solar powered desalination device was studied.

The main limit of this technology is the salt deposit which affects the desalination unit and

its efficiency. In order to avoid so, a boiling regime called film boiling has been studied. Film boiling regime is characterized by a sudden increase in temperature between the heated wall and the fluid being heated. A boiling crisis then takes place, which leads to the formation of a vapor film around the heated surface. This film avoids contact between heated water and the heated wall, thus avoiding salt deposit in the case of seawater boiling.

The experimental set-up made possible the creation of the film. It was also noticed, that once the film was established, the inlet power could be slowly decreased without the film vanishing.

Results also showed that once the film was in place, it created an insulating barrier between water and receiver. This can protect the wall from salt deposit, but also had a clearing effect on already fouled equipment. Regarding the different receivers tested, it was found that copper receivers were more efficient. Their geometry has an impact on their performance. Half-aperture angles of 30 ° and 60 ° showed 1.5 more efficiency than 45 °.

References

[1] N. C. Darre and G. S. Toor. Desalination of Water: a Review. *Current PollutionReports*, 4(2):104–111, June 2018.

[2] M. Ali Abdelkareem, M. El Haj Assad, E. Taha Sayed, and B. Soudan. Recent progress in the use of renewable energy sources to power water desalination plants. *Desalination*, 435:97–113, June 2018.

[3] J. Bundschuh, M. Kaczmarczyk, N. Ghaffour, and B. Tomaszewska. State-of-the-art of renewable energy sources used in water desalination: Present and future prospects. *Desalination*, 508:115035, July 2021.

[4] L. Zhu, L. Sun, H. Zhang, Hu Aslan, Y. Sun, Y. Huang, F. Rosei, and M. Yu. A solution to break the salt barrier for high-rate sustainable solar desalination. *Energy & Environmental Science*, 14(4):2451–2459, 2021.

[5] M. Shahabuddin, M.A. Alim, Tanvir Alam, M. Mofijur, S.F. Ahmed, and G. Perkins. A critical review on the development and challenges of concentrated so- lar power technologies. *Sustainable Energy Technologies and Assessments*, 47: 101434, October 2021.

[6] J. Blanco, E. Zarza, D. Alarcón, S. Malato, and J. León. Advanced Multi-Effect Solar Desalination Technology: The PSA Experience. Solarpaces, Zurich, Switzerland 2002.

[7] Solar Water recovery, generation & reforestation technology. URL https://www.swplc.com/.

[8] D. Lorfing, A. Ahmadi, S. Laborie, R. Olives, Q. Falcoz, X. Py, and L. Tiruta-Barna. Energy and environmental performance of a new solar boiler with heat recovery for seawater desalination. *Sustainable Production and Consump- tion*, 32:330–343, July 2022

[9] D. Lorfing, R. Olives, Q. Falcoz, E. Guillot, C. Le Men, and A. Ahmadi. Design and performance of a new type of boiler using con- centrated solar flux. *Energy Conversion and Management*, 249:114835, December 2021.

[10] Van P. Carey. Liquid Vapor Phase Change Phenomena: An Introduction to the Thermophysics of Vaporization and Condensation Processes in Heat Transfer Equipment, 3rd Edition. CRC Press, 2017